JOURNAL OF BIOMOLECULAR STRUCTURE AND DYNAMICS
https://doi.org/10.1080/07391102.2021.1889668

Taylor & Francis
Taylor & Francis Group

In silico design of novel tubulin binding 9-arylimino derivatives of noscapine, their chemical synthesis and cellular activity as potent anticancer agents against breast cancer

Rajesh Kumar Meher[a], Praveen Kumar Reddy Nagireddy[b], Pratyush Pragyandipta[a], Srinivas Kantevari[b], Satyandra Kumar Singh[c], Vijay Kumar[d] and Pradeep K. Naik[a]

[a]Department of Biotechnology and Bioinformatics, Centre of Excellence in Natural Products and Therapeutics, Sambalpur University, Sambalpur, India; [b]Organic Chemistry Division-II (CPC Division), CSIR-Indian Institute of Chemical Technology, Hyderabad, India; [c]Center For Advance Research, Stem Cell and Tissue Culture Laboratory, King George's Medical University, Lucknow, India; [d]Department of Surgical Oncology, King Georgès Medical University, Lucknow, India

Communicated by Ramaswamy H. Sarma

ABSTRACT

We present a series of 9-arylimino derivatives of noscapine (an antitussive plant alkaloid) that binds to tubulin and displaying anticancer activity against a panel of breast cancer cells. These compounds were rationally designed by coupling of Schiff base containing imine groups at position-9 of the isoquinoline ring of noscapine. Based on a combination of Glide docking and free energy of binding (FEB) calculation, we have screened a panel of three 9-compounds, **12–14** with improved binding affinity with tubulin compared to noscapine. The predicted FEB is −6.166 kcal/mol for **12**, −6.411 kcal/mol for **13** and −7.512 kcal/mol for **14**. In contrast, the predicted FRB of noscapine is −5.135 kcal/mol. These novel derivatives were strategically synthesized and validated their anticancer activity based on cellular studies using two human breast adenocarcinoma, MCF-7 and MDAMB-231, as well as with a panel of primary breast tumor cells isolated from patients. Interestingly, all these derivatives inhibited cellular proliferation in all the cancer cells that ranged between 3.6 and 26.4 μM, which is 11.02–2.03 fold lower than that of noscapine. Unlike previously reported derivatives of noscapine that arrest cells in the S-phase, these novel derivatives effectively inhibit proliferation of cancer cells, arrest the cell cycle in the G2/M-phase and induced apoptosis. Thus, we conclude that 9-arylimino derivatives of noscapine have great potential to be a novel therapeutic agent for breast cancers.

ARTICLE HISTORY
Received 1 November 2020
Accepted 6 February 2021

KEYWORDS
Noscapine; 9-arylimino noscapinoids; tubulin binding; anticancer agents; breast cancer

Introduction

Chemotherapy remains the current method of therapy for metastatic cancer, in that, along with DNA binding drugs, microtubule (MT)-interacting drugs, for example, taxanes, vinca alkaloids, estramustine, halaven and ixempra are utilized for the treatment of localized and metastatic breast cancers. However, these medications possess severe toxicities such as leucocytopenias, diarrhea, alopecia, peripheral neuropathies, etc., resulting in poor quality of life (Kavanagh & Kudelka, 1993; Rowinsky & Donehower, 1991). The wonderful promise of taxol in managing breast cancers justifies further effort to discover novel mitotic inhibitors that may have less side effects and that can be easily administered.

In a quest of finding such molecule, by rational screening of natural compounds, noscapine (an opium alkaloid, non-narcotic, orally available, safe antitussive drug for over 40 years) was discovered. It binds to tubulin heterodimer with a 1:1 stoichiometry, alters the secondary structure of tubulin and arrests the dividing cells at mitosis (Ye et al., 1998). However, the cancer cells selectively undergo apoptosis because of the compromised cell cycle checkpoints, without hampering the normal dividing cells. The careful real-time observation of individual polymerizing MTs *in vitro* and tracking the plus end growth over time revealed that noscapine affected MT-dynamics primarily by enhancing the time period that MTs spend in an attenuated pause state rather than engaging into active depolymerization and repolymerization (Zhou et al., 2002). Because noscapine only affects MT dynamics, cellular functions that do not require exquisite control of MT dynamics may not be interrupted. Noscapine, therefore, has no detectable neurotoxic effect on the histologies of peripheral nerves (Landen et al., 2004). It has favorable pharmacokinetics *in vivo* (clearance within ∼10 h) (Jordan & Wilson, 1998) and has no significant side effects (Ke et al., 2000; Landen et al., 2002). *In vitro* as well as mouse xenograft models have shown that noscapine and its analogs are useful in treatment of cancer of different tissue origin (Ke et al., 2000; Ye et al., 1998; Zhou et al., 2003). These properties enable its therapeutic use at high concentrations (∼150–300 mg/kg body weight) in murine models of

CONTACT Pradeep K. Naik pknaik1973@gmail.com; pknaik1973@suniv.ac.in Centre of Excellence in Natural Products and Therapeutics, Department of Biotechnology and Bioinformatics, Sambalpur University, Jyoti Vihar, Burla, Sambalpur 768019, Odisha, India

Supplemental data for this article can be accessed online at https://doi.org/10.1080/07391102.2021.1889668.

human cancer (Landen et al., 2002; Zhou et al., 2003). It is found to inhibiting proliferation and inducing apoptosis in human ovarian carcinoma cell lines that are sensitive or resistant to paclitaxel (Zhou et al., 2002). The oral bioavailability of noscapine offers further support for its clinical advancement as a novel chemotherapeutic agent (Dahlström et al., 1982). Therefore, noscapine is a promising anticancer drug with minimum toxicity and side effects.

From an ongoing quest to improve our therapeutic arsenal, we have developed a battery of derivatives by modification of its scaffolds and demonstrated to have high tubulin binding and anti-tumor activity compared to noscpine without any debilitating toxicities (Manchukonda et al., 2012, 2013; Naik, Chatterji, et al., 2011; Naik et al., 2012; Santoshi et al., 2011, 2015). While several synthesized derivatives of noscapinoids showed promising *in vitro* activity against a panel of breast tumor cell lines, the antiproliferative activity comes to be in higher concentration (IC_{50}>20 μM). Therefore, there is an urgent need to take up further optimization of noscapine towards development of novel and more promising derivatives. In this study, we approach to develop 9-arylimino congeners of noscapine by strategically modifying its scaffold structure; followed by screening of a panel of most potent derivatives based on our *in silico* efforts. The screened out derivatives were then chemically synthesized and validated for their anticancer activity based on cellular study using two human breast cancer cell lines MCF-7 and MDAMB-231, as well as a panel of primary breast cancer cells directly obtained from breast cancer patients. The novel derivatives were found to bind tubulin heterodimer with increased binding affinity, effectively inhibiting cancer cell proliferation, selectively arrest cancer cells at G2/M phase and induced apoptosis.

Materials and methods

Protein preparation

The crystal structure of amino noscapine-tubulin complex (PDB ID: 6Y6D, resolution 2.20 Å, Oliva et al., 2020) was downloaded from the PDB databank and used for structure-based designing of novel derivatives of noscapine. It was then prepared using protein preparation wizard workflow (Schrödinger, LLC, New York, NY). Further, an all atom molecular dynamics (MD) simulation of 100 ns in explicit water was performed to refine the structure using GROMACS version 4.5.4 (University of Groningen, Netherlands) software (Berendsen et al., 1995) and the GROMOS96 force field with similar parameters as reported earlier (Santoshi & Naik, 2014). Finally, the last 2000 frames from the MD trajectory were used to generate an average structure of the tubulin.

Rational design of 9-arylimino congeners of noscapine

We envisaged developing 9-arylimino derivatives of noscapine by hybridizing with arylimino groups (Schiff bases). It is because; Schiff base analogs have been used in the pharma industry to develop potential analogs for anticancer activity. As an example, Schiff bases obtained from coumarin and pyrazole aldehyde have been tested against cancer cell lines that showed mild anti-cancer activities (Ali et al., 2013). Furthermore, mono and bis-Schiff bases have been reported efficacious against five cancer cell lines (Sondhi et al., 2012). Towards designing the 9-arylimino noscapinoids, we approached to strategically appending the Schiff bases containing imino group at the C-9 position of the noscapine scaffold by *in silico* combinatorial chemistry to develop a library as depicted in Figure 1. The library was then used to screen out a panel of most potent compounds using molecular docking and predictive binding free energy.

Preparation of molecular structure

Molecular structures of noscapinoids (Figure 2) that have been previously reported (Aneja, Vangapandu, Lopus, Chandra, et al., 2006; Manchukonda et al., 2013; Naik, Santoshi, et al., 2011; Santoshi et al., 2011, 2015) and the newly designed 9-arylimino noscapinoids (Figure 1) were built using ChemDraw version 8.00 (California Institute of Technology, USA). These structures were imported into Maestro (Schrödinger, LLC, New York, NY) and were energy minimized using Macromodel (Schrödinger, LLC, New York, NY) and OPLS 2005 force field with PRCG algorithm (energy gradient of 0.001). The molecular structures were further refined through density functional theory (DFT) calculations using hybrid DFT with Becke's three-parameter exchange potential and the Lee-Yang-Parr correlation functional (B3LYP) with basis set 6–31 G** using Jaguar (Schrödinger, LLC, New York, NY). Further, the structural parameters (bond lengths and bond angles) obtained from the DFT calculations for the newly designed compounds were compared with the crystal structure of the noscapine to validate their structure. The structural parameters of the core structure of newly designed molecules and crystal structure of noscapine were almost similar (Supplementary data S1–S3). The appropriate bond order for each structure was defined and their various conformations were generated using Ligprep (Schrödinger, LLC, New York, NY).

Molecular docking

Molecular docking of noscapinoids with αβ-tubulin heterodimer was performed using Glide (Schrödinger, LLC, New York, NY) as reported previously (Naik, Santoshi, et al., 2011). Briefly, a grid box of size 12 Å×12 Å×12 Å was defined at the centroid of the noscapine binding site (Naik, Santoshi, et al., 2011) using Glide grid-receptor generation program. All the noscapinoids were docked using Glide XP (extra precision) and evaluated using a Glide XP_{Score} function. The single best conformation for each ligand was considered for further analysis.

LIE-SGB model building

A predictive model was developed based on linear interaction energy model (LIE) with a surface generalized Born (SGB) continuum solvation model (Zhou et al., 2001) to calculate the free energy of binding (FEB) ($\Delta G_{bind,\ pred}$) of the

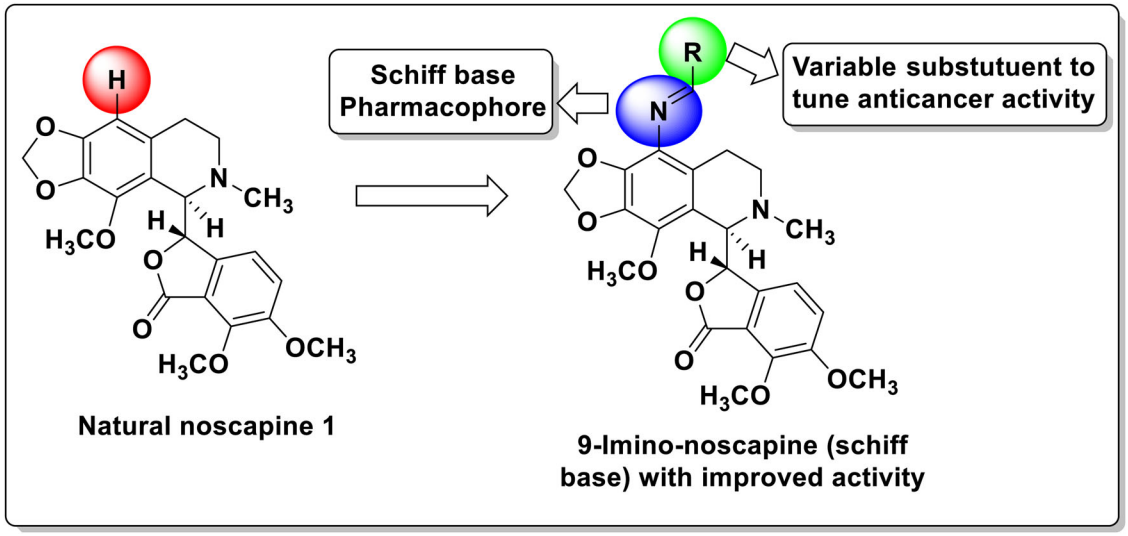

Figure 1. Strategic development of 9-arylimino noscapinoids by hybridizing Schiff base with natural noscapine.

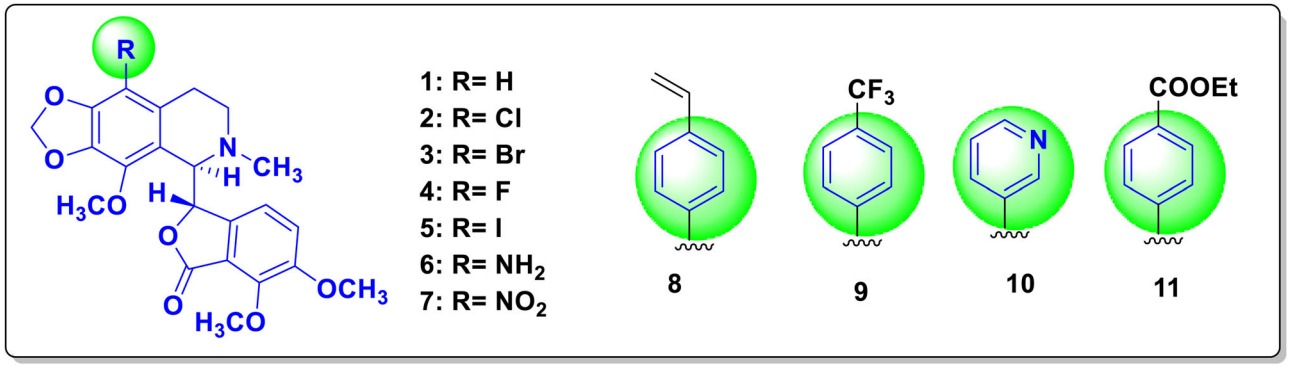

Figure 2. The molecular structure of noscapine and its previously reported derivatives **2–11** used as training set for the molecular modeling study.

newly designed 9-arylimino noscapinoids with tubulin. The training data set of noscapinoids (Figure 2) with known experimental FEB ($\Delta G_{bind,\ expt}$) was used and mapped with various predicted energy parameters such as van der Waals (U_{vdw}), columbic (U_{coul}), reaction field (U_{rxn}) and cavity energy (U_{cav}) based on LIE model to develop the empirical prediction model. The $\Delta G_{bind,expt}$ of noscapinoids with tubulin was calculated from their respective dissociation constant (K_d) values using the relation:

$$\Delta G_{bind,\,expt} = RT\ ln\ K_d$$

where R is gaseous constant (0.001986 kcal/mol) and T is temperature (298 K). Liaison program (Schrödinger, LLC, New York, NY) was used to estimate the above energy parameters from the docked complexes of the noscapinoids based on the Hybrid Monte Carlo simulation technique as reported previously (Santoshi et al., 2015).

$$\Delta G_{bind,\,pred} = \alpha\left(\left\langle U^{b}_{vdw}\right\rangle - \left\langle U^{f}_{vdw}\right\rangle\right) + \beta\left(\left\langle U^{b}_{coul}\right\rangle - \left\langle U^{f}_{coul}\right\rangle\right) + \gamma\left(\left\langle U^{b}_{rxn}\right\rangle - \left\langle U^{f}_{rxn}\right\rangle\right) + \delta\left(\left\langle U^{b}_{cav}\right\rangle - \left\langle U^{f}_{cav}\right\rangle\right)$$

Here $\langle\rangle$ represents the ensemble average, b represents the bound form of the ligand, f represents the free form of the ligand, and α, β, γ and δ are the coefficients of various energy terms, determined using Minitab statistical package (Minitab Inc., State College, PA). Finally based on the docking score and the predictive FEB, we have screened out three most potent 9-arylimino noscapinoids, **12–14** (Figure 3) having enhanced binding affinity with tubulin compared to noscapine for chemical synthesis and cellular evaluation to determine their anticancer potential.

General procedure for chemical synthesis of 9-arylimino noscapinoids, 12–14

The natural α-noscapine was used as a starting material to produce 9-aminonoscapine **6** *via* two reaction steps involving bromination of noscapine using aqueous HBr/Br_2-H_2O followed by amination using CuI, NaN_3 and L-Proline in DMSO as reported earlier (Manchukonda et al., 2012). A solution of 9-aminonoscapine **6** (1.0 mmol), in ethanol (15 mL), was refluxed with substituted aryl/heteroaryl aldehydes (2,5-difluorobenzaldehyde or 5-bromothiophenecarboxaldehyde or p-bromo benzaldehyde, 1.0 mmol), for 12 h. After the starting material was completely consumed in the reaction (judged by TLC), the solvent was evaporated under vacuum. The crude residue was extracted into dichloromethane

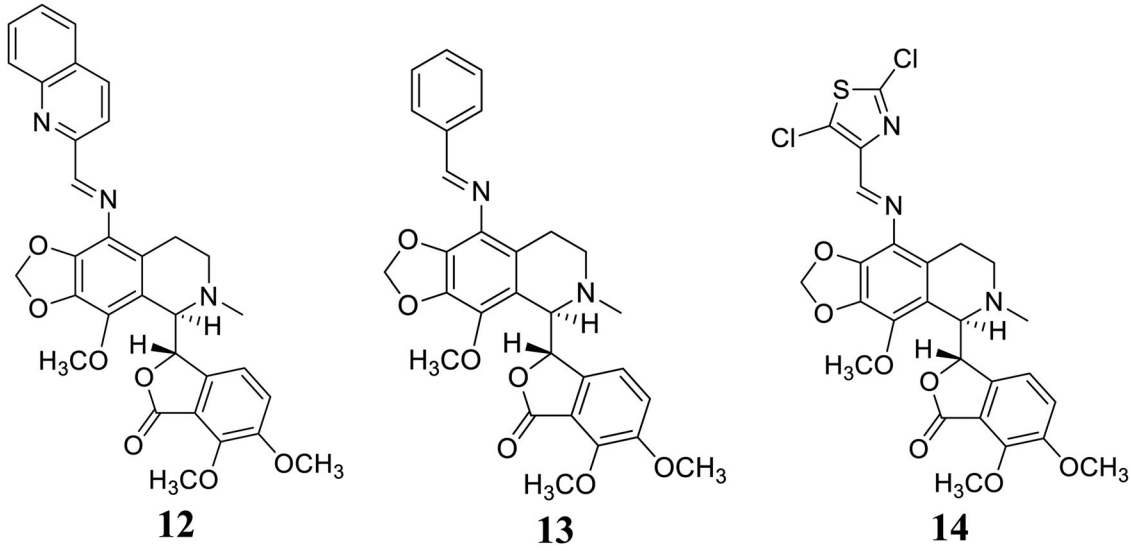

Figure 3. A panel of 9-arylimino noscapinoids, **12–14** that are rationally designed and screened out to have higher binding affinity with tubulin for chemical synthesis and experimental evaluation.

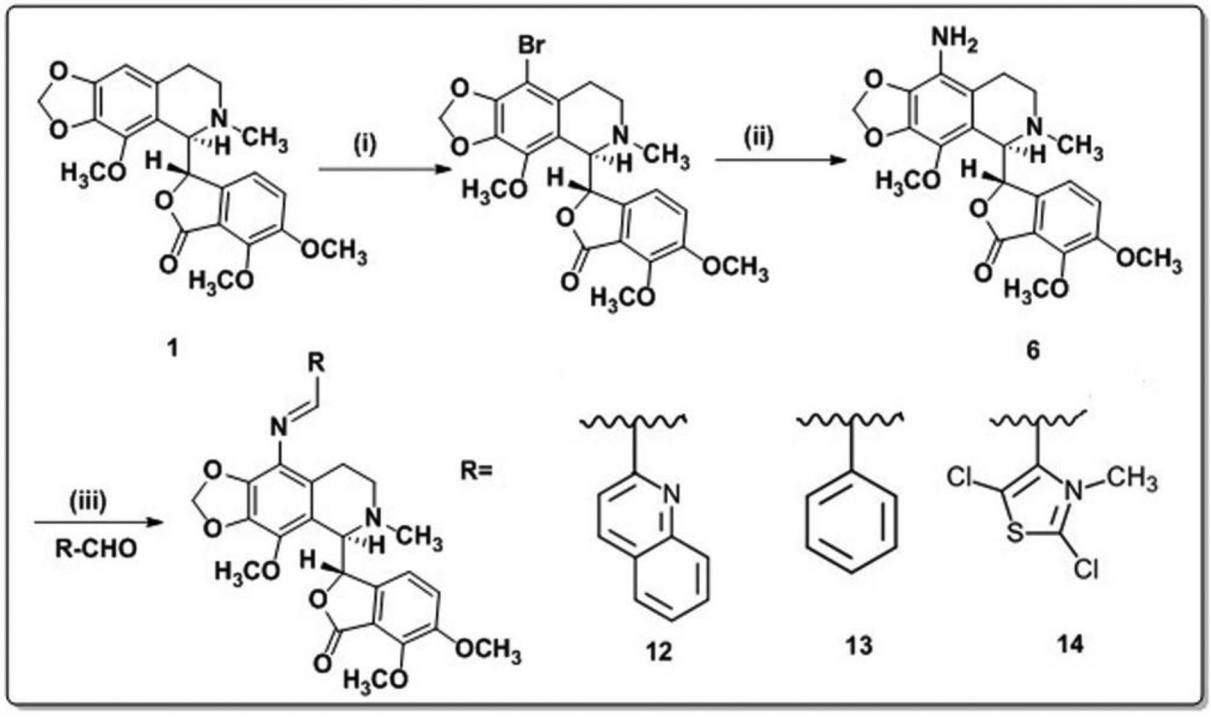

Figure 4. A panel of 9-arylimino noscapinoids, **12–14** that are rationally designed and screened out to have higher binding affinity with tubulin for chemical synthesis and experimental evaluation.

(2 × 15 mL) and washed with brine solution. The organic layer was collected and passed through a Na_2SO_4 bed and later on removed under reduced pressure. The crude residue was chromatographed over a triethylamine silica bed, using pet.ether/ethyl acetate (7:3) as eluents, to produce 9-arylimino noscapinoids, **12–14** as solid products in very good yield (Figure 4). Structural characterization of all the intermediates and final products **12–14** were done using NMR (^{1}H and ^{13}C), IR spectroscopy and mass (HRMS) spectrometry techniques.

Structural characterization of 9-arylimino noscapinoids, 12–14

(S)-6,7-dimethoxy-3-((R)-4-methoxy-6-methyl-9-((E)-(quinolin-3-ylmethylene)amino)-5,6,7,8-tetrahydro-[1,3]dioxolo[4,5-g]isoquinolin-5-yl)isobenzofuran-1(3H)-one (12)

Nature: White solid. TLC (Hexane: Ethylacetate 3:1; Rf: 0.21) M.P: 120–122 °C. IR (KBr): 3446, 2929, 2794, 1757, 1626, 1498, 1443, 1382, 1268, 1036, 1007, 970, 763 cm^{-m}. ^{1}H NMR (400 MHz, $CDCl_3$): δ 9.22 (s, 1H, N = *CH*), 8.35 (d, *J*= 8.5 Hz,

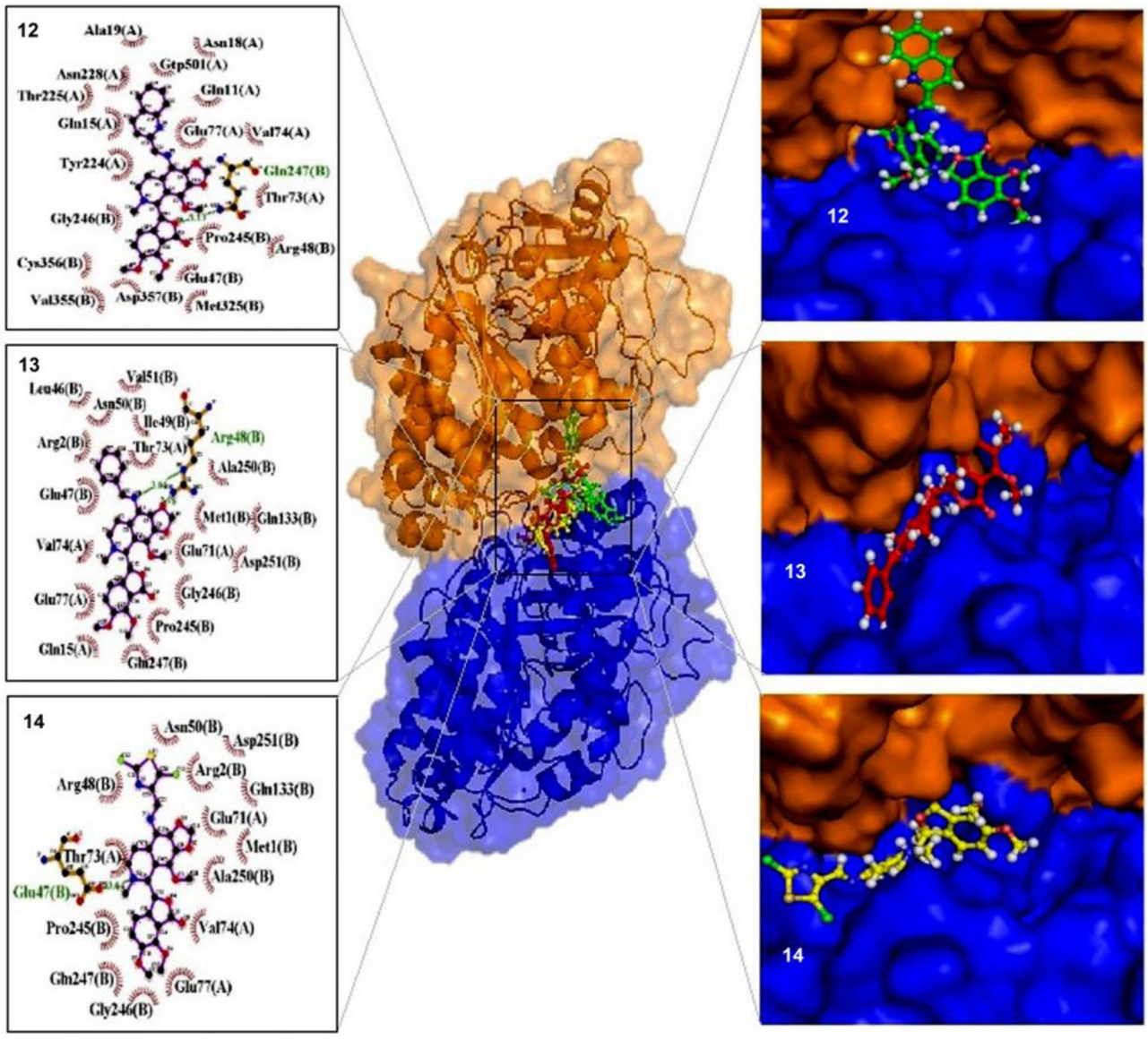

Figure 5. The newly designed 9-arylimino noscapinoids **12–14** are well accommodated inside the noscapine binding site at the interface of α- and β- tubulin. The binding site is represented as macromodel surface according to α- and β- tubulin (α-tubulin is represented in blue color and β-tubulin is represented in brown color). The ligplot analysis showed the interaction of binding site amino acids with the 9-arylimino noscapinoids **12–14**. The binding site residues involved in the interactions are slightly different mainly because of the variation in functional groups. The hydrogen bonds formed (if any) are represented as dotted lines.

1H, Ar-H), 8.23–8.15 (m, 2H, Ar-H), 7.86 (d, *J*= 7.9 Hz, 1H, Ar-H), 7.79–7.74 (m, 1H, Ar-H), 7.62–7.57 (m, 1H, Ar-H), 7.00 (d, *J*= 8.3 Hz, 1H, Ar-H), 6.31 (d, *J*= 8.3 Hz, 1H, Ar-H), 6.04 (d, *J*= 0.9, 17.7 Hz, 2H, O-C*H*$_2$-O), 5.59 (d, *J*= 4.4 Hz, 1H, Ar-H, (C3-phthalide)), 4.42 (d, *J* = 4.4 Hz, 1H, Ar-H, (C5′-isoquinoline)), 4.10 (s, 3H), 4.07 (s, 3H), 3.85 (s, 3H), 3.16–3.06 (m, 1H, -C*H*H-N-CH$_3$ (C7′-isoquinoline)), 2.78–2.70 (m, 1H, -CH*H*-N-CH$_3$ (C7′-isoquinoline)), 2.57 (s, 3H, -N-C*H*$_3$), 2.49–2.40 (m, 1H, Ar-C*H*H (C8′-isoquinoline)), 2.14–2.03 (m, 1H, Ar-CH*H* (C8′-isoquinoline)). ^{13}C NMR (75 MHz, CDCl$_3$): δ 168.0(C = O), 161.8(Ar-C), 155.8(Ar-CH = N-), 152.1(Ar-C), 147.9(Ar-C), 147.6(Ar-C), 141.2(Ar-C), 139.77(Ar-C), 139.72(Ar-C), 136.3(Ar-C), 134.4(Ar-C), 130.1(Ar-C), 129.7(Ar-C), 129.5(Ar-C), 128.7(Ar-C), 127.6(Ar-C), 127.4(Ar-C), 124.5(Ar-C), 119.8(Ar-C), 118.2(Ar-C), 118.0(Ar-C), 117.7(Ar-C), 117.6(Ar-C), 101.1(-O-CH$_2$-O-), 81.7(C-phthalide), 62.2(C- isoquinoline), 60.8(-O-CH$_3$), 59.4(-O-CH$_3$), 56.7(-O-CH$_3$), 49.4(-CH$_2$-), 45.9(N-CH$_3$), 22.9(-CH$_2$-). MS (ESI-MS) *m/z*: 568 [M + H]+ HRMS (ESI): Calculated for $C_{32}H_{30}N_3O_7$ [M + H]+: 568.20783, found: 568.20704.

(S)-3-((R)-9-((E)-benzylideneamino)-4-methoxy-6-methyl-5,6,7,8-tetrahydro [1,3]dioxolo [4,5-g]isoquinolin-5-yl)-6,7-dimethoxyisobenzofuran-1(3H)-one (13)

Nature: White solid. TLC (Hexane: Ethylacetate 3:1; Rf: 0.24) M.P: 88–90 °C. IR (KBr): 3426, 2937, 1759, 1627, 1497, 1385, 1266, 1123, 1034, 756, 693 cm^{-m}. ^{1}H NMR (500 MHz, CDCl$_3$): δ 8.85 (s, 1H, N = C*H*), 7.89 (d, *J*= 3.6 Hz, 2H, Ar-H), 7.50–7.42 (m, 3H, Ar-H), 6.99 (d, *J*= 8.2 Hz, 1H, Ar-H), 6.31 (d, *J*= 8.2 Hz, 1H, Ar-H), 5.99 (d, *J*= 20.44 Hz, 2H, O-C*H*2-O), 5.58 (d, *J*= 4.2 Hz, 1H, Ar-CH, (C3-phthalide)), 4.40 (d, *J*= 4.2 Hz, 1H, Ar-CH, (C5′-isoquinoline)), 4.10 (s, 3H, -OCH3), 4.04 (s, 3H, -OCH3), 3.85 (s, 3H, -OCH$_3$), 3.02–2.94 (m, 1H, -C*H*H-*N*-CH$_3$ (C7′-isoquinoline)), 2.72–2.65 (m, 1H, -CH*H*-*N*-CH$_3$ (C7′-

isoquinoline)), 2.55 (s, 3H, *N*-CH_3), 2.44–2.36 (m, 1H, Ar-C*H*H (C8′-isoquinoline)), 2.06–1.97 (m, 1H, Ar-CH*H* (C8′-isoquinoline)). ^{13}C NMR (100 MHz, $CDCl_3$): δ 168.1(C = O), 161.8(Ar-C), 152.1(Ar-CH = N-), 147.6(Ar-C), 141.3(Ar-C), 141.1(Ar-C), 139.0(Ar-C), 138.7(Ar-C), 136.9(Ar-C), 134.5(Ar-C), 131.1(Ar-C), 129.0(Ar-C), 128.6(Ar-C), 128.3(Ar-C), 125.7(Ar-C), 119.8 (Ar-C), 118.3(Ar-C), 117.7(Ar-C), 117.6(Ar-C), 100.8(-O-CH_2-O-), 81.8(C-phthalide), 62.2(C-isoquinoline), 60.9(-O-CH_3), 59.5(-O-CH_3), 56.7(-O-CH_3), 49.4(-CH_2-), 45.9(N-CH_3), 22.7(-CH_2-). MS (ESI-MS) *m/z*: 517 [M + H]+ HRMS (ESI): Calculated for $C_{29}H_{29}N_2O_7$ [M + H]+: 517.19693, found: 519.19596.

(S)-3-((R)-9-((E)-((2,4-dichlorothiazol-5-yl)methylene)amino)-4-methoxy-6-methyl-5,6,7,8-tetrahydro[1,3]dioxolo[4,5-g]isoquinolin-5-yl)-6,7-dimethoxyisobenzofuran-1(3H)-one(14)

Nature: White solid. TLC (Hexane: Ethylacetate 3:1; Rf: 0.26) M.P: 107–109 °C. IR (KBr): 3451, 2932, 1758, 1622, 1499, 1404, 1267, 1066, 1033, 897, 735 cm^{-m}. ^{1}H NMR (500 MHz, $CDCl_3$): δ 8.97 (s, 1H, N = CH), 7.02 (d, *J*= 8.2 Hz, 1H, Ar-H), 6.39 (d, *J*= 8.2 Hz, 1H, Ar-H), 6.04 (dd, *J*= 1.0, 16.3 Hz, 2H, O-CH_2-O), 5.53 (d, *J*= 4.4 Hz, 1H, Ar-CH, (C3-phthalide)), 4.36 (d, *J*= 4.4 Hz, 1H, Ar-CH, (C5′- isoquinoline)), 4.10 (s, 3H, -OCH_3), 4.02 (s, 3H, -OCH_3), 3.87 (s, 3H, -OCH_3), 2.96-2.89 (m, 1H, -C*H*H-*N*-CH_3 (C7′-isoquinoline)), 2.80–2.73 (m, 1H, -CH*H*-*N*-CH3 (C7′-isoquinoline)), 2.53 (s, 3H, NC*H*3), 2.47–2.39 (m, 1H, Ar-C*H*H (C8′-isoquinoline)), 2.09–2.01 (m, 1H, Ar-CH*H* (C8′-isoquinoline)). ^{13}C NMR (100 MHz, $CDCl_3$): δ 167.9(C = O), 154.2(Ar-C), 152.2(Ar-CH = N-), 149.2(Ar-C), 147.6(Ar-C), 141.3(Ar-C), 140.1(Ar-C), 139.8(Ar-C), 138.0(Ar-C), 134.8(Ar-C), 134.2(Ar-C), 130.2(Ar-C), 123.6C(Ar-C), 119.6(Ar-C), 118.4(Ar-C), 117.8(Ar-C), 117.5(Ar-C), 101.2(-O-CH_2-O-), 81.5(C-phthalide), 62.2(C-isoquinoline), 60.8(-OCH_3), 59.4(-OCH_3), 56.7(-OCH_3), 48.9(-CH_2-), 45.5(N-CH_3), 22.3(-CH_2-). MS (ESI-MS) *m/z*: 592 [M + H]+ HRMS (ESI): Calculated for $C_{26}H_{24}Cl_2N_3O_7$ [M + H]+: 592.07065, found: 592.07031.

Cell culture and reagents

Noscapine was obtained from Sigma. All the chemical reagents and media for cell culture were obtained from Sigma. Human breast cancer cell line, MCF-7 and MDAMB-231 were obtained from the cell repository of the National Centre for Cell Science Pune, Maharashtra, India. Primary breast cancer cells (PBCs) were isolated from the patient's samples. Stock solution (100 mM) of the newly synthesized 9-arylimino noscapinoids, **12–14** was prepared with dimethyl sulfoxide (DMSO) and stored at 4 °C until use. The cells were allowed to grow at a temperature of 37 °C in a 5% CO_2 and 95% humidity in Dulbecco's modified Eagle medium (DMEM), supplemented with 10% fetal bovine serum (FBS) and antibiotics. Cells with a 70-80% confluence were subcultured for bioassays using trypsin-EDTA (0.25%).

In vitro cell proliferation assay using MCF-7 and MDAMB-231 cell lines

Antiproliferation activity of 9-arylimino noscapinoids, **12–14** was performed in 96-well plates as described previously (Naik, Santoshi, et al., 2011) using two human breast cancer cell lines, MCF-7 and MDAMB-231. In brief, cells were grown in DMEM culture medium supplemented with 10% FBS, 1% penicillin/streptomycin and 2 mM l-glutamine at 37 °C in a humidified atmosphere with 5% CO_2. Cells were plated at a density of 5×10^3 cells per well and were treated with gradient concentrations (5–100 μM) of noscapine and its derivatives, 9-arylimino noscapinoids, **12–14** for 72 h. The cells were then fixed with 50% trichloroacetic acid and stained with 0.4% sulforhodamine B (SRB). The unbound dye was removed by washing. The protein-bound dye was then extracted with 10 mM Tris base and measured the optical density at 564 nm using a SPECTRAmax PLUS 384 microplate spectrophotometer. The IC_{50} value that stands for the drug concentration required to achieve a cell kill of 50% was determined using the online tool Quest GraphTM IC_{50} Calculator (AAT Bioquest, Inc., Sunnyvale, CA, https://www.aatbio.com/tools/ic50-calculator). The experiment was repeated for three times.

Primary breast cancer cells (PBCs) culture and in vitro cell proliferation assay

PBCs were isolated from the patient's samples (8 nos.) with different stages of breast cancer before drug treatment in aseptic condition. The tumor tissues were treated with 0.25% trypsin and filtered with 70 μm filter followed by centrifugation at 2000 rpm for 3 min with serum-free medium. The filtered cells were collected and plated in T25 flask and incubated with complete DMEM culture medium, supplemented with 10% FBS and 1% pentrip (mixture of penicillin and streptomycin) at 37 °C under 5% CO_2. Fresh media was replaced every 3–4 d, and subsequent passages were performed under the same conditions as mentioned above. The cultured were maintained for homogeneous cell type at subconfluence between 3 and 8 passages. Cells were allowed to reach 80–90% confluence prior to experimental treatments. After the confluence reached, the primary cells were plated at 2000 cells/well in 96 wells plate with culture media. The cells were maintained at 37 °C in a humidified atmosphere with 5% CO_2 and were treated with gradient concentrations (5–100 μM) of noscapine and 9-arylimino noscapinoids, **12–14** for 72 h. Measurement of cell proliferation was performed by SRB assay, using the CellTiter96 AQueous One Solution Reagent (Sigma, St. Louis, MO). Cells were stained with SRB for 30 min. The unbound dye was removed by washing. The bound dye was extracted with 1 mM tris and absorbance was measured using a SPECTRAmax PLUS 384 microplate spectrophotometer at 564 nm. The percentage of cell survival as a function of drug concentration was plotted and the IC_{50} value was determined using the online tool, AAT Bioquest. The experiment was repeated three times.

Flow cytometry analysis of cell cycle progression

Inhibition of cell cycle progression with the treatment of 9-arylimino noscapinoids was investigated using MDAMB-231 cells. The cells were maintained in DMEM culture media with 4.5 g/L glucose and L-glutamine supplemented with 10% FBS and 1% penicillin/streptomycin, at 37 °C in a 5% CO_2 atmosphere. After reaching the 80–90% confluence, cells were treated with noscapine and 9-arylimino noscapinoids, **12–14** dissolved in 1% phosphate buffer saline (PBS). After 72 h of treatment, cells were harvested and analyzed using flow cytometry. Briefly, 2×10^6 cells were centrifuged, washed twice with ice-cold PBS and fixed in 70% ethanol at −20 °C for 24 h. The cells were centrifuged at 1000 × *g* for 10 min and the supernatant was discarded. The pellet was resuspended in 30 µL of phosphate/citrate buffer (0.2 M Na_2HPO_4/0.1 M citric acid, pH 7.5) at room temperature for 30 min. The cells were washed with 5 mL of PBS, incubated with 0.5 mL of propidium iodide (20 µg/mL in 0.6% Triton-X in PBS) and 0.5 mL of RNase A (20 µg/mL in PBS) for 45 min. in dark. Samples were analyzed on a flow cytometer (BD FACS Aria-III) and the progress in the cell cycle was determined.

Flow cytometry analysis for apoptosis assay

Apoptosis in cancer cells was detected by Annexin-V-FITC apoptosis detection method by using Apoptosis detection kit (Sigma-Aldrich, St. Louis, MO) based on instruction provided by manufacture. For experimental purpose 3×10^4 cells per well were seeded on 12 well culture plate and incubated for 24 h with complete medium. The cells were treated with IC_{50} concentration of noscapine and 9-arylimino noscapinoids, **12–14** and were harvested at 72 h. Cells were typsinized and stained with surface marker antibodies (biotin-conjugated Annexin V, FITC-conjugated streptavidin) and propiumdium iodide (PI). Cells were allowed to suspend in 1X binding buffer and incubated with Annexin V FITC conjugate for 20 min in dark condition at room temperature. Flow cytometer data with 488 nm excitation for PI and emission at 530 nm were collected. Viable cells (Annexin V^-/PI^-), early apoptotic cells (Annexin V^+/PI^-), late apoptotic/necrotic cells (Annexin V^+/PI^+) and late necrotic cells (Annexin V^-/PI^+) were identified and determined their percentage.

Results and discussion

After the establishment of anticancer activity of the lead molecule, noscapine, several derivatives have been developed by various groups in order to increase its therapeutic outcome. Many of these derivatives were demonstrated to have higher binding affinity with tubulin, antiproliferative activity and induction of apoptosis. As an example the tubulin-binding affinity and antiproliferative activity have been increased to 20–80 folds by developing halogenated, nitro, amino and biaryl noscapinoids by modification at C-9 position of the scaffold (Aneja, Vangapandu, Lopus, Chandra, et al., 2006; Aneja, Vangapandu, Lopus, Viswesarappa, et al., 2006; Naik et al., 2012; Santoshi et al., 2015) as well as by functionalization of 'N' in isoquinoline unit of natural α-noscapine (Jain et al., 2011). Structure-activity data of these derivatives of noscapine led us to develop a reasonable predictive model for predicting the FEB of newly designed derivatives and screening of promising derivatives. We are reporting in this study a panel of 9-arylimino noscapinoids, **12–14** as potent anticancer agents.

Docking score of designed noscapinoids with tubulin

The molecular interaction and binding affinities of designed noscapinods, **12–14** onto tubulin were calculated applying molecular docking in combination with LIE-SGB empirical modeling. Noscapinoids, previously reported (Figure 2) and newly designed in this study (Figure 3) were docked into the noscapinoids binding site (Naik, Santoshi, et al., 2011; Oliva et al., 2020) using Glide XP (extra precision) and evaluated using a Glide XP_{score} function (Friesner et al., 2004; Halgren et al., 2004). The three 9-arylimino noscapinoids, **12–14,** which revealed better docking scores ranging from −8.466 kcal/mol to −6.085 kcal/mol than the parent compound, noscapine (−5.505 kcal/mol) were finally screened out. All the three noscapinoids docked well at the interface of α- and β- tubulin (Figure 5). Their mode of interaction with the binding site amino acids is depicted as ligplot (Figure 5). The ligplot explains the formation of different hydrogen bonds and hydrophobic interactions between the ligands and the binding site amino acids.

Predictive binding affinity of 9-arylimino noscapinoids, 12–14 with tubulin (LIE-SGB calculation)

The binding affinity ($\Delta G_{bind,pred}$) of 9-arylimino noscapinoids, **12–14** with tubulin was predicted based on computationally developed LIE, utilizing the experimental activity of training set molecules (Table 1). Since the molecular docking predicts accurate binding pose for the ligands onto the receptor, we have used the docking complexes of noscapinoids with tubulin and performed hybrid Monte Carlo simulation with generalized Born (SGB) continuum solvation model to calculate the various interaction energy terms (van der Waals energy (U_{vdw}), Columbic energy (U_{coul}), reaction energy (U_{rxn}) and cavity energy (U_{cav})) using liaison (Schrodinger). These energy parameters of the training set molecules (Table 1) were mapped with their $\Delta G_{bind,expt}$ based on LIE model to develop the robust prediction model for predicting the $\Delta G_{bind,pred}$ of the noscapinoids with tubulin. The values obtained for the four fitting parameters, α, β, γ and δ are 0.08446, −0.00223, −0.000872 and −0.45601, respectively. The $\Delta G_{bind,pred}$ of the training set molecules based on LIE-SGB model is very close to the $\Delta G_{bind,expt}$ (root mean square error was 0.243 kcal/mol) (Table 1). The quality of the fit can also be judged by the value of the squared correlation coefficient (R^2) and analysis of variance (F-value).

$$\Delta G_{bind,pred} = 0.08446\langle U_{vdw}\rangle - 0.00223\langle U_{coul}\rangle - 0.00872\langle U_{rxn}\rangle - 0.45601\langle U_{cav}\rangle$$

($n = 11$, $R^2 = 0.998$, $s = 0.243$, $F = 3742.6$, $p \leq .001$)

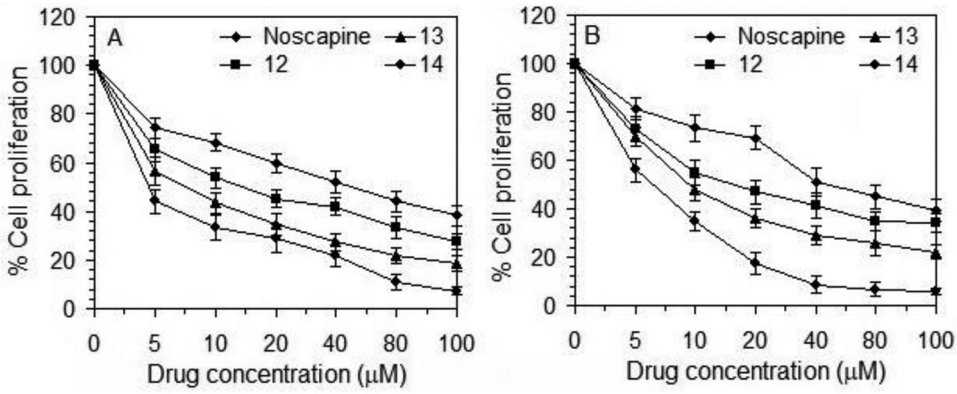

Figure 6. The 9-arylimino noscapinoids **12–14** are more active compared to noscapine in inhibiting the proliferation of human breast cancer cells. Both (A) MCF-7 and (B) MDAMB-231cells were treated with noscapine and 9-arylimino noscapinoids, **12–14** for 72 h. Each value represents the average of three independent experiments.

Table 1. Molecular docking results (Glide XP) as well as calculated energies using Liasion programme (Schrodinger package) of noscapine and its derivatives: van der Waals energy (U_{vdw}), Columbic energy (U_{coul}), reaction energy (U_{rxn}) and cavity energy (U_{cav}) as well as predicted binding free energy ($\Delta G_{bind,pred}$) based on LIE-SGB prediction model and experimental binding free energy ($\Delta G_{bind,expt}$).

Ligand	Glide XP_{score} (kcal/mol)	$<U_{vdw}>$ (kcal/mol)	$<U_{coul}>$ (kcal/mol)	$<U_{rxn}>$ (kcal/mol)	$<U_{cav}>$ (kcal/mol)	Experimental ΔG_{bind} (kcal/mol)	Predicted ΔG_{bind} (kcal/mol)
1	−1.927	−45.14	−330.8	135.5	2.097	−5.246	−5.212
2	−2.038	−49.00	−210.2	116.0	3.283	−6.006	−6.178
3	−2.766	−42.50	−362.1	155.9	4.208	−5.827	−6.060
4	−2.940	−48.06	−355.8	168.7	2.548	−5.587	−5.899
5	−3.263	−47.69	−285.7	135.5	3.103	−6.360	−5.987
6	−4.492	−47.44	−77.3	118.2	3.954	−6.628	−6.668
7	−2.605	−33.39	−331.9	176.7	4.465	−5.551	−5.657
8	−2.287	−45.57	−277.9	112.3	3.285	−5.665	−5.706
9	−2.350	−33.47	−324.5	152.5	3.766	−5.783	−5.151
10	−3.679	−45.41	−471.2	152.8	3.669	−5.673	−5.790
11	−4.687	−42.69	−267.6	129.9	3.465	−5.518	−5.722
12	−6.031	−42.73	−373.1	180.6	3.976	–	−6.166
13	−2.862	−45.81	−317.4	150.1	4.602	–	−6.411
14	−3.001	−47.26	−277.2	169.3	6.092	–	−7.512

The newly designed 9-arylimino noscapinoids, **12–14** revealed improved $\Delta G_{bind,pred}$ compared to the lead molecule, noscapine. $<U_{vdw}>$, $<U_{coul}>$, $<U_{rxn}>$ and $<U_{cav}>$ energy terms represents the ensemble average energy terms calculated as the difference between bound and free state of the ligands and its environment.

Because of high predictability, the LIE-SGB model was used to predict the $\Delta G_{bind,pred}$ of the newly designed 9-arylimino noscapinoids, **12–14,** which revealed improved predicted binding energy of −6.166 kcal/mol for **12**, −6.411 kcal/mol for **13** and −7.512 kcal/mol for **14**, respectively, in comparison to the lead molecule (−5.135 kcal/mol) were chemically synthesized for experimental evaluation.

9-Arylimino noscapinoids, 12–14 inhibits proliferation of MCF-7 and MDAMB-231

Based on our *in silico* results, we focused at the cellular level to determine if the 9-arylimino noscapinoids, **12–14,** affected cancer cell proliferation. All the 3 compounds including the parent compound, noscapine were analyzed for their antiproliferative activity in two human breast cancer cell lines, MCF-7 (estrogen- and progesterone-receptor positive) and MDAMB-231 (estrogen- and progesterone-receptor negative). The IC_{50} values for the compounds for both the cell lines are collated in Table 2. The 9-arylimino noscapinoids, **12–14** exhibited potent cytotoxic activity in comparison to noscapine using both the cell lines (Figure 6). The IC_{50} value amounted to 44.5, 16.0, 7.1 and 3.6 μM for noscapine, 1**2, 13** and **14**, respectively, for MCF-7 cells, which reflects a modest antiproliferative activity. Parenthetically, a similar modest IC_{50} value of 53.1, 20.5, 11.2 and 6.0 μM was measured for noscapine, **12, 13** and **14**, respectively, for MDAMB-231 cells. The differences in IC_{50} values obtained using MCF-7 and MDAMB-231 for these 9-arylimino noscapinoids were cell-type dependent. Although a significant correlation on the sensitivity of cancer cells to these analogues cannot yet be established at this stage, it is evident, that tubulin represents a potential target for these compounds.

Table 2. IC_{50} values of novel 9-arylimino noscapinoids, **12–14** using two human breast adenocarcinoma cell lines, MCF-7 and MDAMB-231.

	IC_{50} (μM)			
	Noscapine	12	13	14
MCF-7	44.5 ± 4.8	16.0 ± 2.7	7.1 ± 1.3	3.6 ± 0.8
MDA-MB-231	53.1 ± 4.5	20.5 ± 2.9	11.2 ± 1.6	6.0 ± 1.2

All the novel derivatives were found to have improved antiproliferative activity compared to noscapine.

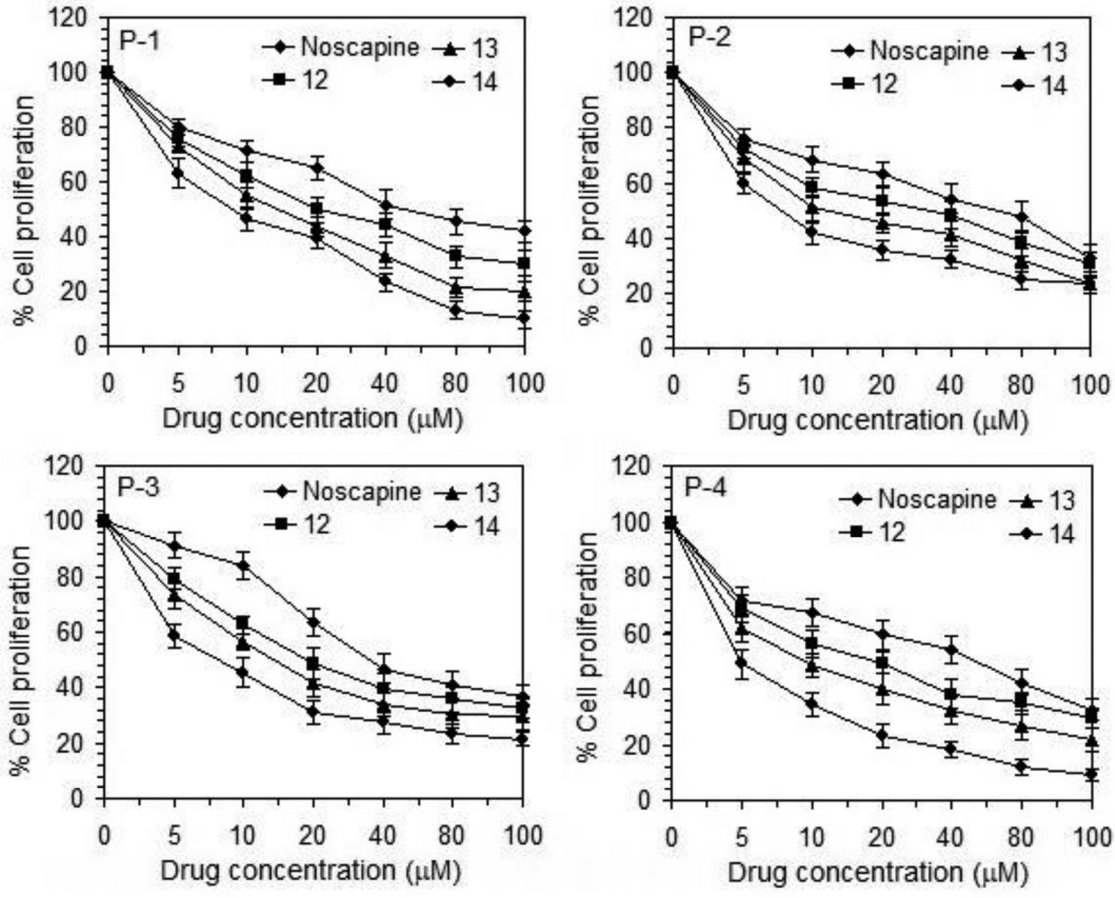

Figure 7. The 9-arylimino noscapinoids, **12–14** are more active compared to noscapine in inhibiting the proliferation of a panel of human primary breast cancer cells. All the cells treated with 9-arylimino noscapinoids, **12–14** for 72 h. Each value represents the average of three independent experiments.

9-Arylimino noscapinoids, 12–14 inhibits proliferation of primary breast cancer cells

Further, we tested the antiproliferation activity of 9-arylimino noscapinoids, **12–14** using a panel of primary breast tumor cells. We have obtained the surgically removed breast tumor samples from 08 different patients with different stages of breast cancer and processed the samples to isolate the primary tumor cells. All these primary breast tumor cells were treated with increasing concentrations of the noscapinoids to determine their IC_{50} value. The IC_{50} values for the test compounds are collated in Table 3. The IC_{50} value ranges from 39.7 to 53.8 μM for noscapine, 17.2–26.4 μM for **12**, 9.7–16.4 μM for **13** and 4.4–9.5 μM for **14** using a panel of primary breast cancer cells (Table 3). All the 9-arylimino noscapinoids developed exhibited potent cytotoxic activity in comparison to noscapine using all the primary breast cancer cells (Figure 7).

9-Arylimino noscapinoids, 12–14 induced apoptosis to cancer cells

We approached to determine the induction of apoptotic cell death to breast cancer cell by the newly developed 9-arylimino noscapinoids, **12–14**. Biochemically the apoptotic process is characterized by alterations of lipid composition of cell membrane – phosphatidylserine which is normally on the inner leaflet of the cell membrane, translocates to the outer leaflet, which can be measured fluorescently by annexin V binding. In contrast, a cell-impermeant DNA-binding fluorescent dye, propodium iodide can only enter the cells when it is at the stage of late apoptosis when membrane permeability is compromised. The apoptotic cells can be quantified in large extent by FACS analysis. The percentage of early apoptotic and late apoptotic cells using MDAMB-231 cell lines for the treatment of noscapine and its 9-arylimino noscapinoids, **12–14** with a concentration of 25 μM for 72 h is collated in Table 4. Representative Figs of flow cytometry analysis with treatment of noscapine and its 9-arylimino noscapinoids, **12–14** are included in Figure 8. After 72 h of culture, the control untreated cell culture contained only very few early apoptotic (2.5%) and late apoptotic cells (1.0%), which were considered as the background cell death due to regular trauma during cell culture (Table 4). In contrast, the percentage of early apoptotic cells of 15%, 45%, 56% and 5% as well as late apoptotic cells of 30%, 3%, 4% and 35% with treatments of noscapine and its 9-arylimino noscapinoids, **12–14**, respectively, was found to be significantly high compared to controlled untreated cells (Table 4).

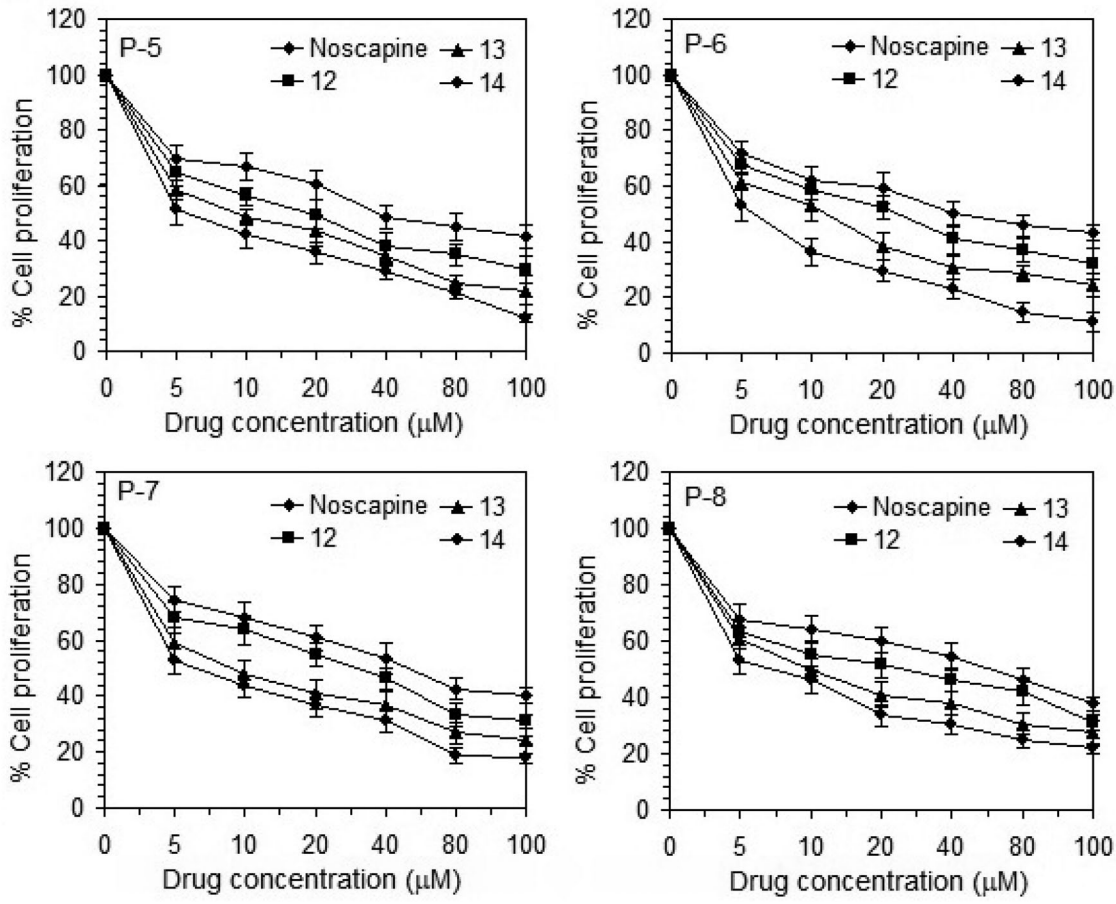

Figure 7. (Continued).

Table 3. IC_{50} values of novel 9-arylimino noscapinoids, **12–14** using primary breast cancer cells isolated from breast tumor tissue of different patients.

	IC_{50} (μM)			
Patients no.	Noscapine	12	13	14
1	53.8 ± 5.3	24.4 ± 2.9	14.9 ± 2.4	9.5 ± 0.7
2	47.1 ± 5.7	26.4 ± 2.6	15.6 ± 1.8	7.5 ± 0.5
3	43.8 ± 4.8	24.3 ± 2.7	16.4 ± 2.3	7.3 ± 0.8
4	39.7 ± 4.3	18.6 ± 2.3	10.2 ± 1.3	4.4 ± 0.4
5	44.6 ± 4.9	17.2 ± 2.2	9.9 ± 1.5	5.9 ± 0.6
6	47.0 ± 4.5	21.9 ± 3.1	11.0 ± 1.7	5.3 ± 0.3
7	46.9 ± 4.8	25.9 ± 3.5	9.7 ± 0.8	6.4 ± 0.5
8	46.3 ± 5.2	21.7 ± 2.6	11.1 ± 0.6	6.4 ± 0.4

All the novel derivatives were found to have improved antiproliferative activity compared to noscapine.

Cell cycle profile and mitotic arrest of cancer cells at G_2/M phase with treatment of noscapinoids

To ensure the induction of cell death, we examined the effect of noscapine and 9-arylimino noscapinoids, **12–14** (25 μM concentration) on the cell cycle profile of MDAMB-231 based on FACS analysis and represented in Figure 9. Fluorescently labeled DNA accumulation is a good pointer of cell cycle profile and cell death. Cells with 2 N DNA represent the G1 phase, while cells with duplicated 4 N DNA represent G2 and M phases. Cells in the process of DNA duplication with 2 N and 4 N peaks represent S phase when DNA is being synthesized. Less than 2 N DNA appears in populations of dying cells that degrade their DNA to different extents. Treatment of MDAMB-231 cells for 72 h with the test compounds led to significant perturbations of the cell cycle profile at 25 μM. FACS analysis revealed high accumulation of cells in the G2M phase at 72 h of treatment of noscapine and its 9-arylimino derivatives compared to untreated cells (Table 5). In contrast to G2M block, a characteristic hypodiploid DNA content peak (sub-G1) was seen to rise at 72 h of treatment. The progressive generation of cells having hypodiploid DNA content reflects fragmented DNA, indicating dying cells.

Conclusion

In conclusion, we have strategically designed a panel of 9-imine-noscapinoids of natural lead molecule, noscapine in quest of accelerating its anticancer activity. We have also provided simplest methods for the direct and regioselective modification of noscapine scaffold to produce the 9-arylimino derivatives in high yields. All the three 9-arylimino noscapinoids, **12–14** developed have showed increase antiproliferative activity to cancer cells based on our extensive

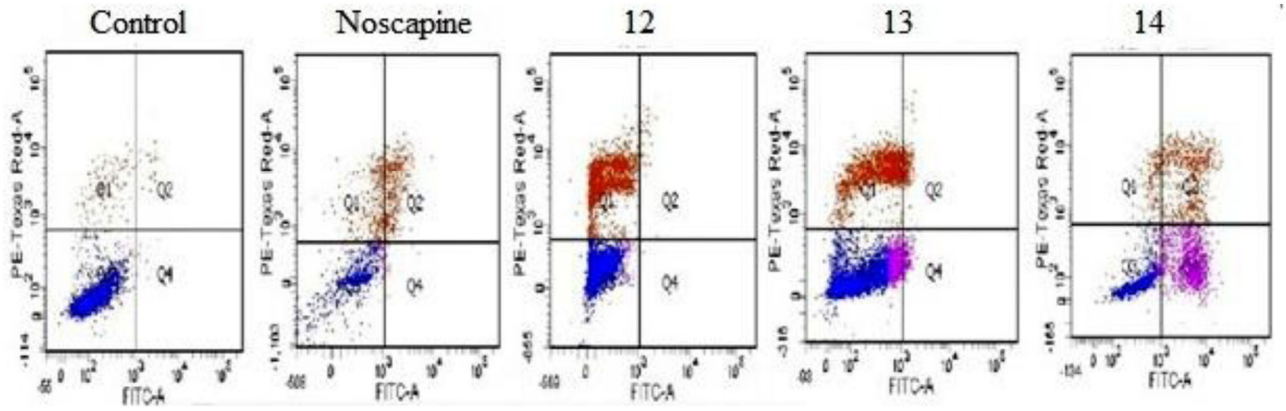

Figure 8. Flow cytometry analysis of phosphatidylserine (PS) exposure in MDAMB-231 cells treated with noscapine and its 9-arylimino noscapinoids, **12–14** with 25 μM for 72 h and compared with non-treated control cells. Annexin-V and propidium iodide (PI) were used to distinguish among three sub-populations of cells: PI- and Annexin V– cells represent viable cells with intact membrane and preserved amino-phospholipid asymmetry, PI- and Annexin V + cells represent early apoptotic cells with intact cellular membrane exposing phosphatidylserine, whereas PI + and Annexin V + cells represent late apoptotic cells with compromised asymmetry and membrane permeability. Representative results of three independent experiments.

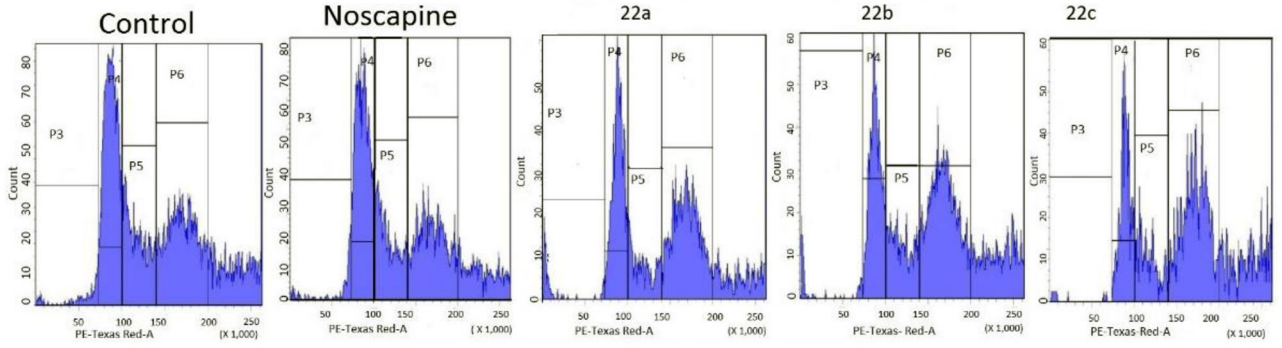

Figure 9. Noscapine and its 9-arylimino derivatives inhibit cell cycle progression at mitosis followed by the appearance of a characteristic hypodiploid (sub-G1) DNA peak, indicative of apoptosis. Panels A–E depict analyses of cell cycle profile, determined by flow cytometry using MDAMB-231 cells treated with 25 μM concentration of noscapine and its derivatives at 72 h of treatment.

Table 4. Percentage of viable (Q3), early apoptotic (Q1), late apoptotic (Q2) and necrotic (Q4) cell measured by flow cytometry.

Viability/Apoptotic	Control (%)	Noscapine (%)	12 (%)	13 (%)	14 (%)
Q1	2.5	15	45	56	5
Q2	1	30	3	4	35
Q3	94	50	50	35	15
Q4	0.5	1	2	3	45

Table 5. Effect of noscapine and its 9-arylimino noscapinoids, **12–14** on cell cycle profile of MDAMB-231 cells treated with 25 μM solution for 72 h.

	72 h			
	Sub-G_1	G_0/G_1	S	G_2/M
Control	0.9	9	14	7.2
Noscapine	3.2	11.8	9.7	13.8
12	5.3	13.2	8.2	19.7
13	7.5	12.7	11.2	32.6
14	8.9	14.2	10.1	37.3

molecular modeling and cellular study using two human breast cancer cell lines, MCF-7 and MDAMB-231 as well as a panel of primary breast cancer cells. Therefore, these novel compounds may prove efficacious not only in the treatment of breast carcinoma, but also for other type of cancers. Our results compel us to continue to examine the effects of these novel compounds on *in vivo* animal experiment with the final goal of taking it to the human clinical study.

Acknowledgments

We would like to acknowledge the financial support provided by the OHEPEE, Govt. of Odisha, through World Bank under Centre of Excellence in Natural Products and Therapeutics, Sambalpur University. Rajesh Kumar Meher wishes to acknowledge the award of student research fellowship (DST/INSPIRE/Code No.: IF160351).

Disclosure statement

The authors declare that they have no competing financial interests or personal relationships that could have appeared to influence the work reported in this article.

Funding

This work was supported by OHEPEE, Govt. of Odisha, through World Bank under Centre of Excellence in Natural Products and Therapeutics and Department of Science and Technology, Govt. of India for the fellowship to Mr. Rajesh Kumar Meher.

References

Ali, I., Haque, A., Saleem, K., & Hsieh, M. F. (2013). Curcumin-I Knoevenagel's condensates and their Schiff's bases as anticancer

agents: Synthesis, pharmacological and simulation studies. *Bioorganic & Medicinal Chemistry*, *21*(13), 3808–3820. https://doi.org/10.1016/j.bmc.2013.04.018

Aneja, R., Vangapandu, S. N., Lopus, M., Chandra, R., Panda, D., & Joshi, H. C. (2006). Development of a novel nitro-derivative of noscapine for the potential treatment of drug-resistant ovarian cancer and T-cell lymphoma. *Molecular Pharmacology*, *69*(6), 1801–1809. https://doi.org/10.1124/mol.105.021899

Aneja, R., Vangapandu, S. N., Lopus, M., Viswesarappa, V. G., Dhiman, N., Verma, A., Chandra, R., Panda, D., & Joshi, H. C. (2006). Synthesis of microtubule-interfering halogenated noscapine analogs that perturb mitosis in cancer cells followed by cell death. *Biochemical Pharmacology*, *72*(4), 415–426. https://doi.org/10.1016/j.bcp.2006.05.004

Berendsen, H. J., van der Spoel, D., & van Drunen, R. (1995). GROMACS: A message-passing parallel molecular dynamics implementation. *Computer Physics Communications*, *91*(1–3), 43–56. https://doi.org/10.1016/0010-4655(95)00042-E

Dahlström, B., Mellstrand, T., Löfdahl, C. G., & Johansson, M. (1982). Pharmacokinetic properties of noscapine. *European Journal of Clinical Pharmacology*, *22*(6), 535–539. https://doi.org/10.1007/BF00609627

Friesner, R. A., Banks, J. L., Murphy, R. B., Halgren, T. A., Klicic, J. J., Mainz, D. T., Repasky, M. P., Knoll, E. H., Shelley, M., Perry, J. K., Shaw, D. E., Francis, P., & Shenkin, P. S. (2004). Glide: A new approach for rapid, accurate docking and scoring. 1. Method and assessment of docking accuracy. *Journal of Medicinal Chemistry*, *47*(7), 1739–1749. https://doi.org/10.1021/jm0306430

Halgren, T. A., Murphy, R. B., Friesner, R. A., Beard, H. S., Frye, L. L., Pollard, W. T., & Banks, J. L. (2004). Glide: A new approach for rapid, accurate docking and scoring. 2. Enrichment factors in database screening. *Journal of Medicinal Chemistry*, *47*(7), 1750–1759. https://doi.org/10.1021/jm030644s

Jain, N., Yada, D., Shaik, T. B., Vasantha, G., Reddy, P. S., Kalivendi, S. V., & Sreedhar, B. (2011). Synthesis and antitumor evaluation of nitrovinyl biphenyls: Anticancer agents based on allocolchicines. *ChemMedChem*, *6*(5), 859–868. https://doi.org/10.1002/cmdc.201100019

Jordan, M. A., & Wilson, L. (1998). The use and action of drugs in analyzing mitosis. *Methods in cell biology* (Vol. 61, pp. 267–295). Academic Press. https://doi.org/10.1016/s0091-679x(08)61986-x

Kavanagh, J. J., & Kudelka, A. P. (1993). Systemic therapy for gynecologic cancer. *Current Opinion in Oncology*, *5*(5), 891–899. https://doi.org/10.1097/00001622-199309000-00019

Ke, Y., Ye, K., Grossniklaus, H. E., Archer, D. R., Joshi, H. C., & Kapp, J. A. (2000). Noscapine inhibits tumor growth with little toxicity to normal tissues or inhibition of immune responses. *Cancer Immunology, Immunotherapy: CII*, *49*(4–5), 217–225. https://doi.org/10.1007/s002620000109

Landen, J. W., Hau, V., Wang, M., Davis, T., Ciliax, B., Wainer, B. H., Van Meir, E. G., Glass, J. D., Joshi, H. C., & Archer, D. R. (2004). Noscapine crosses the blood-brain barrier and inhibits glioblastoma growth. *Clinical Cancer Research*, *10*(15), 5187–5201. https://doi.org/10.1158/1078-0432.CCR-04-0360

Landen, J. W., Lang, R., McMahon, S. J., Rusan, N. M., Yvon, A. M., Adams, A. W., Sorcinelli, M. D., Campbell, R., Bonaccorsi, P., Ansel, J. C., Archer, D. R., Wadsworth, P., Armstrong, C. A., & Joshi, H. C. (2002). Noscapine alters microtubule dynamics in living cells and inhibits the progression of melanoma. *Cancer Research*, *62*(14), 4109–4114.

Manchukonda, N. K., Naik, P. K., Santoshi, S., Lopus, M., Joseph, S., Sridhar, B., & Kantevari, S. (2013). Rational design, synthesis, and biological evaluation of third generation α-noscapine analogues as potent tubulin binding anti-cancer agents. *PLoS One*, *8*(10), e77970. https://doi.org/10.1371/journal.pone.0077970

Manchukonda, N. K., Sridhar, B., Naik, P. K., Joshi, H. C., & Kantevari, S. (2012). Copper(I) mediated facile synthesis of potent tubulin polymerization inhibitor, 9-amino-α-noscapine from natural α-noscapine. *Bioorganic & Medicinal Chemistry Letters*, *22*(8), 2983–2987. https://doi.org/10.1016/j.bmcl.2012.02.033

Naik, P. K., Chatterji, B. P., Vangapandu, S. N., Aneja, R., Chandra, R., Kanteveri, S., & Joshi, H. C. (2011). Rational design, synthesis and biological evaluations of amino-noscapine: A high affinity tubulin-binding noscapinoid. *Journal of Computer-Aided Molecular Design*, *25*(5), 443–454. https://doi.org/10.1007/s10822-011-9430-4

Naik, P. K., Lopus, M., Aneja, R., Vangapandu, S. N., & Joshi, H. C. (2012). In silico inspired design and synthesis of a novel tubulin-binding anticancer drug: Folate conjugated noscapine (Targetin). *Journal of Computer-Aided Molecular Design*, *26*(2), 233–247. https://doi.org/10.1007/s10822-011-9508-z

Naik, P. K., Santoshi, S., Rai, A., & Joshi, H. C. (2011). Molecular modelling and competition binding study of Br-noscapine and colchicine provide insight into noscapinoid-tubulin binding site. *Journal of Molecular Graphics & Modelling*, *29*(7), 947–955. https://doi.org/10.1016/j.jmgm.2011.03.004

Oliva, M. A., Prota, A. E., Rodríguez, S. J., Bennani, Y. L., Jiménez, B. J., Bargsten, K., Canales, A., Steinmetz, M. O., & Díaz, J. F. (2020). Structural basis of noscapine activation for tubulin binding. *Journal of Medicinal Chemistry*, *63*(15), 8495–8501. https://doi.org/10.1021/acs.jmedchem.0c00855

Rowinsky, E. K., & Donehower, R. C. (1991). The clinical pharmacology and use of antimicrotubule agents in cancer chemotherapeutics. *Pharmacology & Therapeutics*, *52*(1), 35–84. https://doi.org/10.1016/0163-7258(91)90086-2

Santoshi, S., & Naik, P. K. (2014). Molecular insight of isotypes specific β-tubulin interaction of tubulin heterodimer with noscapinoids. *Journal of Computer-Aided Molecular Design*, *28*(7), 751–763. https://doi.org/10.1007/s10822-014-9756-9

Santoshi, S., Manchukonda, N. K., Suri, C., Sharma, M., Sridhar, B., Joseph, S., Lopus, M., Kantevari, S., Baitharu, I., & Naik, P. K. (2015). Rational design of biaryl pharmacophore inserted noscapine derivatives as potent tubulin binding anticancer agents. *Journal of Computer-Aided Molecular Design*, *29*(3), 249–270. https://doi.org/10.1007/s10822-014-9820-5

Santoshi, S., Naik, P. K., & Joshi, H. C. (2011). Rational design of novel anti-microtubule agent (9-azido-noscapine) from quantitative structure activity relationship (QSAR) evaluation of noscapinoids. *Journal of Biomolecular Screening*, *16*(9), 1047–1058. https://doi.org/10.1177/1087057111418654

Sondhi, S. M., Arya, S., Rani, R., Kumar, N., & Roy, P. (2012). Synthesis, anti-inflammatory and anticancer activity evaluation of some mono- and bis-Schiff's bases. *Medicinal Chemistry Research*, *21*(11), 3620–3628. https://doi.org/10.1007/s00044-011-9899-3

Ye, K., Ke, Y., Keshava, N., Shanks, J., Kapp, J. A., Tekmal, R. R., Petros, J., & Joshi, H. C. (1998). Opium alkaloid noscapine is an antitumor agent that arrests metaphase and induces apoptosis in dividing cells. *Proceedings of the National Academy of Sciences of the United States of America*, *95*(4), 1601–1606. https://doi.org/10.1073/pnas.95.4.1601

Zhou, J., Gupta, K., Aggarwal, S., Aneja, R., Chandra, R., Panda, D., & Joshi, H. C. (2003). Brominated derivatives of noscapine are potent microtubule-interfering agents that perturb mitosis and inhibit cell proliferation. *Molecular Pharmacology*, *63*(4), 799–807. https://doi.org/10.1124/mol.63.4.799

Zhou, J., Gupta, K., Yao, J., Ye, K., Panda, D., Giannakakou, P., & Joshi, H. C. (2002). Paclitaxel-resistant human ovarian cancer cells undergo c-Jun NH2-terminal kinase-mediated apoptosis in response to noscapine. *The Journal of Biological Chemistry*, *277*(42), 39777–39785. https://doi.org/10.1074/jbc.M203927200

Zhou, R., Friesner, R. A., Ghosh, A., Rizzo, R. C., Jorgensen, W. L., & Levy, R. M. (2001). New linear interaction method for binding affinity calculations using a continuum solvent model. *The Journal of Physical Chemistry B*, *105*(42), 10388–10397. https://doi.org/10.1021/jp011480z